Research Article

Nano Biomed Eng

Facile Green Synthesis of Ag/AgCl Nanocomposite Using Durian Shell Extract and its Activity Against Methicillin-Resistant *Staphylococcus Aureus*

Thi Anh Thu Nguyen[1], Thi My Thao Nguyen[1], Thi Thanh Le Trinh[1], Phung Anh Nguyen[2], Van Minh Nguyen[3], Nhat Linh Duong[3], Trung Dang-Bao[4], Nguyen Tri[2,3]

[1]School of Applied Chemistry, Tra Vinh University, Tra Vinh City, Vietnam
[2]Institute of Chemical Technology, Vietnam Academy of Science and Technology, Ho Chi Minh City, Vietnam
[3]Faculty of Biotechnology, Ho Chi Minh City Open University, Ho Chi Minh City, Vietnam
[4]Faculty of Chemical Engineering, Ho Chi Minh City University of Technology, VNU-HCM, Ho Chi Minh City, Vietnam

Corresponding authors. E-mail: ntri@ict.vast.vn; dbtrung@hcmut.edu.vn

Received: Sep. 25, 2021; **Revised:** Sep. 21, 2022; **Accepted:** Nov. 14, 2022; **Published:** Nov. 30, 2022

Citation: T.A.T. Nguyen, T.M.T. Nguyen, T.T.L. Trinh, et al. Facile green synthesis of Ag/AgCl nanocomposite using durian shell extract and its activity against methicillin-resistant *staphylococcus aureus*. *Nano Biomedicine and Engineering*., 2022, 14(3): 225–235.
DOI: 10.5101/nbe.v14i3.p225–235

Abstract

The green synthesis of Ag/AgCl nanocomposite using the durian shell extract was carried out under the sunlight illumination at room temperature, showing the face-centered cubic crystalline structures of both Ag and AgCl with nanosizes in the range of 15–25 nm. The high negative potential value of the Ag/AgCl solution (–21.1 mV) established the high dispersion of Ag/AgCl, long-term stability, and good colloidal nature. The antibacterial activity of Ag/AgCl nanocomposite against methicillin-resistant *Staphylococcus aureus* (MRSA) bacteria was highly appreciated with average inhibition zone diameter of 12.0 mm, minimum inhibitory concentration of 8.27 mg/L, and minimum bactericidal concentration of 66.1 mg/L. The present work designed a cost-effective, convenient, eco-friendly protocol to synthesize Ag/AgCl nanocomposite and its efficient antibacterial activity against MRSA was evidenced as well.

Keywords: Green synthesis; Ag/AgCl; Nanocomposite; Durian shell extract; Antibiotic-resistant bacteria

Introduction

Antibiotic resistance of drug-resistant bacteria is one of the severe problems of concern, especially in developing countries. Infectious diseases such as respiratory and gastrointestinal, sexually transmitted, and nosocomial infections account for a high proportion of the disease structure in such countries [1]. However, the antibiotic resistance dramatically decreases efficiency in clinical practice, even the antibiotics being used to treat the patient do not kill the pathogenic bacteria [2]; as a consequence, millions of patients pass away from multidrug-resistant bacteria every year. Apparently, a real burden for governments could be foreseen as the high costs of updated antibiotics to replace the old ones. Drug-resistant bacteria such as methicillin-resistant *Staphylococcus aureus* (MRSA), extended-spectrum β-lactamases (ESBL)-secreting bacteria, carbapenem-resistant *Escherichia coli* (CREC), etc., are markedly

increasing with diverse strains [3, 4]. The formation of drug-resistant bacteria is mainly based on the three mechanisms: (1) limiting the penetration of antibiotics, (2) destroying antibiotics, and (3) inactivating antibiotics. In fact, all types of bacteria have their solutions to limit the penetration of antibiotics into the cell; therefore, antibiotics have less chance to inhibit bacteria. Bacteria increase the stability of the protective film or use the push-pull mechanism on the cell to get out of the antibiotic, resulting in limiting the antibiotics activity. Besides, some groups of bacteria will select to secrete enzymes to destroy antibiotics [5], as observed on intestinal bacteria such as *Staphylococcus aureus*, *Klebsiella sp.*, *Escherichia coli*, etc [6]. Typically, the β-lactamase enzyme can break the lactam ring of the antibiotic. More recently, the antibiotic inactivation has been discovered with mutations in the chromosomes of bacterial cells. Bacteria can block or modify the targets of antibiotics on their cells, thereby causing ineffective drugs. This mechanism usually occurs in gram-positive bacteria (typically MRSA) and rarely in gram-negative bacteria. Because of increasing resistance to methicillin, penicillin, and many other β-lactam antibiotics, MRSA has been considered as one of the most prominent resistant bacteria [3]. Therefore, new bactericidal agents with new mechanisms are always paid a great attention to replace conventional antibiotics.

The effectiveness of metal-based nanoparticles against bacterial strains has been proven, typically gold, silver, copper, etc. [7, 8]. First of all, bacterial cell death caused by the releasing metal ions has been well perceived. Apart from interfering the metabolic system, the heavy metal ions could induce a Fenton reaction to generate reactive oxygen species (ROS) to damage DNA, protein and cell membranes [9, 10]. On the other hand, nanoparticles (NPs) provide extra favourable functions such as physical and electrostatic interaction with cell walls, disruption of the cell external layer, and increased permeability of the cellular membrane. This leads to more efficient microbe killing capability [11], in which, many antibiotic-resistant bacteria showed a low resistance towards silver nanoparticles (AgNPs) [12]; AgNPs penetrated bacterial cells disrupted the membrane/cell wall of drug-resistant bacteria, thereby inhibiting aerobic respiration and destroying deoxyribonucleic acid (DNA), proteins, disrupting bacterial biosynthesis bacteria and destroying them [13]. In comparison with traditional antibiotics, AgNPs in antibacterial can be more effective as it stays in the body for a longer time, promising their antibacterial applications in medicine.

Chlorine radicals and chlorinated compounds are also known for their antibacterial and medical applications [14]. Besides, the combination of Ag^+ and Cl^- radicals could enhance antibacterial effects [14]. Chlorine radicals are very chemically flexible and moderately oxidizing, which can react with various biological components of the bacterial cell. Meanwhile, silver ions with medium oxidizing capacity can bind with the thiol groups (-SH) of many enzymes and bacterial proteins [14]; hence, they destroy such enzymes and proteins in the bacterial cell. Therefore, the synergistic effect of silver and chlorine has brought the interests in studying their antibacterial ability.

Biosynthesis of Ag-based nanoparticles has been widely reported, mainly using plant extracts (coming from stems, leaves, fruits, pods, and bark) [15–18]. The biomolecules involving polyphenols, amino acids, enzymes, tannins, proteins, phenolics, terpenoids, alkaloids, polysaccharides, flavonoids, etc., provoke the reduction of Ag^+ ions to Ag^0 [19]. As the king of fruits in Southeast Asia, the consumption of durian is rising, generating a big amount of its shell as an agricultural residue. Durian shell contains many polysaccharides, which are long chains of carbohydrates consisting of D-galacturonic acid and neutral sugars such as L-rhamnose, L-arabinose, D-galactose, D-glucose, and D-fructose [20, 21], acting as highly efficient reducing agents for the synthesis of AgNPs and Ag-based nanomaterials.

In this study, Ag/AgCl nanocomposite was synthesized by the reduction of $AgNO_3$ solution using durian shell extract as a reducing agent under direct sunlight conditions. The influences of the synthesis duration, the volume ratio of $AgNO_3$ solution/Durian shell extract, and the $AgNO_3$ concentration on Ag/AgCl formation were evaluated. The antibacterial activity of Ag/AgCl nanocomposite was assessed against MRSA by the inhibition zone test, the minimum inhibitory concentration (MIC), and the minimum bactericidal concentration (MBC).

Experimental

Materials

Durian shell (DS) was collected in Tien Giang Province (Vietnam). The raw material was washed, cut into small pieces, and then dried at 60 °C overnight. The extraction process was carried out with a DS

powder/deionized water mass ratio of 1:50 at 80 °C for 1 h. After filtering, the DS extract was stored at 4 °C for the further experiments.

Green synthesis and characterization of Ag/AgCl nanocomposite

Silver nitrate ($AgNO_3$ mass percentage is >99.8%) was purchased from Merck and directly used without purifications. $AgNO_3$ solution was blended with the DS extract under stirring at 300 r/min at room temperature, under sunlight illumination [22, 23]. The effects of the synthesis duration, the volume ratio of $AgNO_3$ solution/DS extract, and the $AgNO_3$ concentration on the Ag/AgCl nanocomposite formation were investigated to achieve the optimal synthetic conditions.

UV-Vis spectrometer (UV-1800, Shimadzu) was used to monitor Ag/AgCl formation at 200–800 nm (measured samples were diluted five times). The crystalline phase of powder Ag/AgCl composite was studied by X-ray diffraction (XRD) using a Bruker D2 Phaser powder diffractometer. The presence of phytochemicals of the DS extracts on the Ag/AgCl surface was confirmed by Fourier transform infrared spectroscopy (FT-IR), performed on an active Tensor 27-Bruker spectrometer in the range 400–4000 cm^{-1}. The morphology of Ag/AgCl composite was characterized by transmission electron microscopy (TEM) using the JEOL JEM2100 instrument, scanning electron microscopy (SEM) and energy-dispersive X-ray spectroscopy (EDS) on JEOL JST-IT 200 instrument. Electrochemical equilibrium on the surfaces and molecular vibrations was determined through zeta potential spectroscopy using a Specifica Horiba SZ-100 instrument.

Antibacterial activity

The Ag/AgCl nanocomposite fabricated at the optimal conditions has been tested for antibacterial activity against MRSA by the inhibition zone test, the MIC, and the MBC, as shown in our previous study [24, 25]. In this study, MRSA ATCC 43300 was provided by Nam Khoa Co., Ltd., Vietnam. The assay of anti-MRSA of Ag/AgCl was performed by using well diffusion method. The MRSA of 10^8 colony forming units per milliliter (CFU/ml) was spread in disc of Mueller-Hinton agar (MHA). Then, a hole with a diameter of about 6 mm is punched aseptically with a sterile cork borer or a tip, and 100 μL of Ag/AgCl solution is introduced into the well. The petri dishes are incubated under suitable conditions of 37 °C for 18–24 h. The antimicrobial agent diffuses in the agar medium and inhibits the growth of the microbial strain tested. Then, the zone of inhibition was determined by measuring the diameter of clear zone. To investigate the MIC of Ag/AgCl against MRSA, the different concentrations of Ag/AgCl (*N*/2, *N*/4, *N*/8, *N*/16, *N*/32, *N*/64, and *N*/128, with *N* = 132.2 mg/L, as the initial concentration of Ag/AgCl solution in deionized water) were prepared by diluting Ag/AgCl solution with deionized water. Afterward, the sterile nutrient agar was mixed with the diluted samples. The standardized inoculum of MRSA with 10^6 CFU/mL was inoculated on agar plates, mixed with Ag/AgCl from low to high concentrations by using sterile sticks. A sterile nutrient agar plate was not mixed with Ag/AgCl as a control. Ultimately, the plates were incubated at 37 °C for 24 h. The lowest concentration of Ag/AgCl that inhibited the growth of MRSA was regarded as the MIC. In the MBC test, bacterial growth inhibitory was used to determine the MBC. Different concentrations of Ag/AgCl were diluted similarly to the MIC method. Then, 200 μL of the sample was spread onto the nutrient agar plate; samples were incubated at 37 °C for 24 h to observe the survival of MRSA bacteria. The MBC value is the lowest concentration that can completely inhibit MRSA bacteria.

Fabrication, characterization, and antibacterial activity testing of Ag/AgCl nanocomposite are illustrated in Fig. 1.

Results and Discussion

Green synthesis and characterization of Ag/AgCl nanocomposite

UV-Vis spectrum of the sample in the dark condition (during 120 min) showed the unchanged absorbance, proving no formation of AgNPs. In contrast, under light illumination for 30 min, the Ag/AgCl nanocomposite formation was discovered with the observed surface plasmon resonance in the wavelength range of 400–450 nm (Fig. 2(a)), described as follows:

$$Ag^+ + H_2O \xrightarrow{hv} Ag^0 + H^+ + OH^*, \quad (1)$$

$$Ag^+ + ROH \xrightarrow{hv} Ag^0 + H^+ + RO^*, \quad (2)$$

$$Ag^+ + RCl \xrightarrow{hv} AgCl + R^+, \quad (3)$$

$$Ag^0 + AgCl \rightarrow Ag/AgCl. \quad (4)$$

The mechanism can be evidenced from the FT-IR spectra, showing the involvement of OH— groups and chlorine contents in the DS extract in the Ag/AgCl synthesis. When increasing the reaction time from 30 to 150 min, the absorbance bands of Ag/

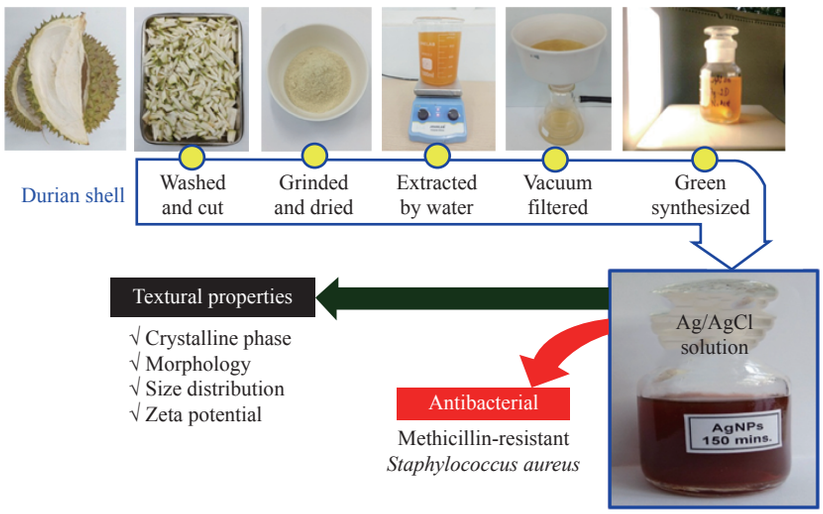

Fig. 1 Schematic illustration of the experimental process

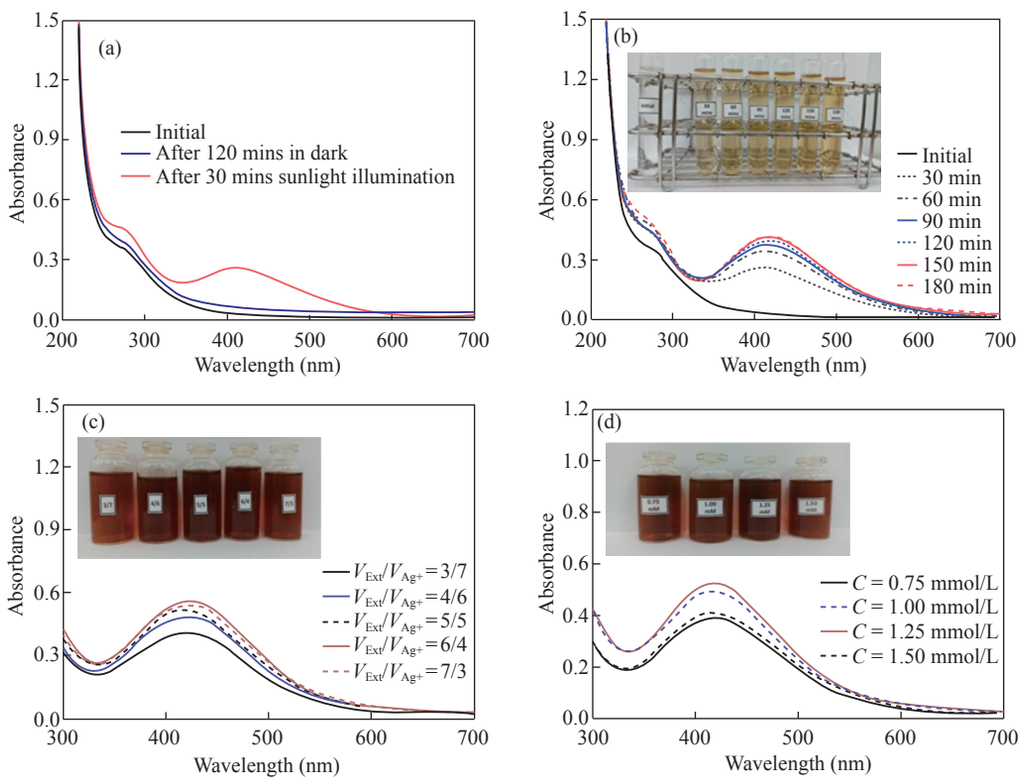

Fig. 2 UV-Vis spectra of Ag/AgCl solutions under various conditions. **(a)** Effect of light illumination; **(b)** Synthesis duration; **(c)** V_{Ext}/V_{Ag+} volume ratio; **(d)** $AgNO_3$ concentration

AgCl nanocomposite increased sharply. After 150 min, the formation of Ag/AgCl nanoparticles was almost completed, with the unchanged maximum absorbance (Fig. 2(b)). The color change from white to dark brown also confirmed the Ag/AgCl formation. The color of the solutions darkened with the reaction time; within 150−180 min, the solution color was almost unchanged. Therefore, 150 min was chosen to investigate further conditions. The highest absorbance of Ag/AgCl was reached with the volume ratio of extract/$AgNO_3$ of 6/4 (Fig. 2(c)). The lower the extract concentration is, the lower the reducing agent/Ag^+ ion ratio is; therefore, fewer Ag^+ ions were reduced and fewer biomolecules were capped on Ag NPs, leading to the larger nanoparticles. With a higher DS extract/$AgNO_3$ ratio, the reduction of Ag^+ ions to Ag0 was more efficient, thus preventing their incorporation into larger-sized nanoparticles. The Ag/AgCl formation rate also increased with increasing Ag^+ concentration [26]. However, the newly formed Ag NPs can be aggregated at high Ag^+ ion concentrations, forming larger-sized particles (Fig. 2(d)). In short, the study determined the

optimal conditions for Ag/AgCl synthesis using the DS extract as reducing agents involving the synthesis time of 150 min, the volume ratio of DS extract/$AgNO_3$ solution of 6/4, and 1.25 mmol/L $AgNO_3$ concentration at room temperature under light illumination.

The physico-chemical properties of Ag/AgCl materials synthesized under the optimal conditions were characterized, including XRD, SEM, TEM, Zeta potential, FT-IR, EDS mapping, and EDX analysis. The crystalline phase of Ag/AgCl was examined by XRD (Fig. 3(a)), showing the five distinct diffraction peaks at 2θ = 38.4°, 44.5°, 64.8°, and 77.9° corresponding to the (111), (200), (220), and (311) planes of the face-centered cubic structure of Ag NPs (JCPDS card No. 89-3722). Besides, the presence of AgCl was confirmed at 2θ = 28.1°, 32.3°, 46.3°, 54.8°, 57.6°, 67.5° and 76.7° with corresponding lattice planes of (111), (200), (220), (311), (222), (400), and (420) of face-centered cubic phase of AgCl (JCPDS card No. 31-1238). The formation of AgCl at room temperature is attributed to the reaction between Ag^+ from $AgNO_3$ and Cl^- from phytochemical compounds in the DS extract [27]. The average crystal size of Ag/AgCl nanocomposites estimated by the Debye-Scherrer formula [28] was about 15.4 nm.

The SEM and TEM images established the spherical Ag/AgCl nanocomposite with particle size ranges of 20−50 nm (Fig. 3(b)) and 15−25 nm (Fig. 3(c)), respectively. The TEM result clearly indicated a thin layer of biomolecules in DS extract surrounding the nanocomposite, preventing the agglomeration and thus stabilizing of Ag/AgCl nanocomposites [29]. In comparison with the TEM image, the bigger Ag/AgCl clusters was observed on the SEM image, probably caused by the sample preparation [30]. The size distribution confirmed the particle diameter of 18.2 nm with the highest occurrence (Fig. 3(d)), being consistent with the TEM and XRD analyses. The electrostatic charge on the surface at the double layer surrounding the Ag/AgCl nanocomposites was measured using Zeta potential, showing the value zeta potential of −21.1 mV (Fig. 4(a)). In fact, the nanoparticles are highly stable in the solution, if the density of negative or positive charges at the surface of Ag/AgCl nanocomposites is lower than −20 mV or higher than 20 mV [31, 32]. The elemental compositions were investigated by EDS mapping (Fig. 4(b)), proving the formation of Ag/AgCl nanocomposite with the appearance of Ag and Cl at the same entities. The signals of O and C in the EDX spectrum (Fig. 4(c)) were attributed to the presence of phytochemical compounds of the DS extract or using carbon tape as a substrate.

The FT-IR spectrum of the powder Ag/AgCl composite (Fig. 5) showed the sharp peaks at 529 and 618 cm^{-1} of the C—Cl group of alkyl halides, the peaks at 869 and 1085 cm^{-1} corresponding to the C—H group

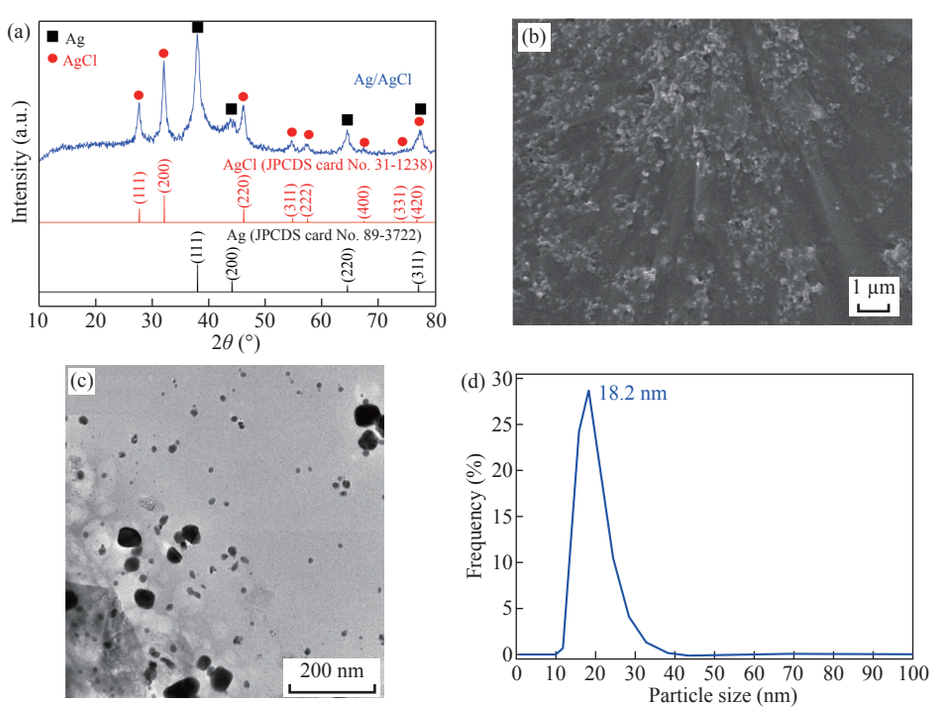

Fig. 3 (a) XRD pattern; **(b)** SEM image; **(c)** TEM image; **(d)** Size distribution of Ag/AgCl synthesized at the optimal conditions

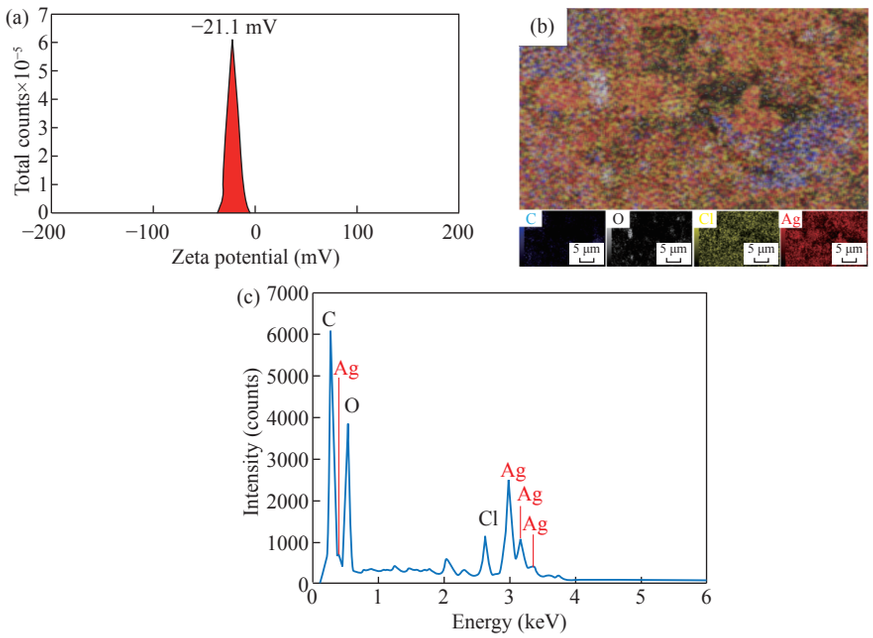

Fig. 4 (a) Zeta potential; **(b)** EDS mapping; **(c)** EDX spectrum of Ag/AgCl synthesized at the optimal conditions

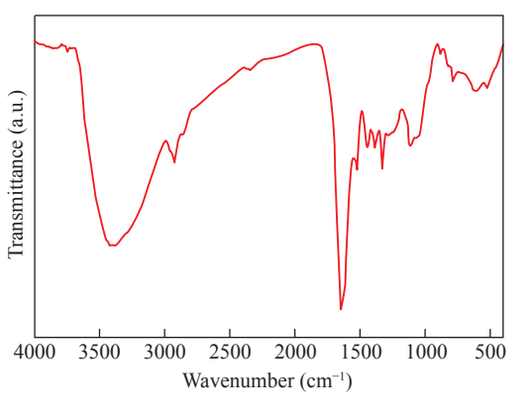

Fig. 5 FT-IR spectrum of powder Ag/AgCl synthesized at the optimal conditions and then dried at 60 °C for 24 h

of the aromatic compounds and the C—N from the amines; the peak at 1440 cm^{-1} of the C—O vibration of the carboxylic acid (—COOH); the peak at 1632 cm^{-1} of a C═C aromatic bond or amide regions attributed to proteins and enzymes; and the peak at 3450 cm^{-1} corresponding to the O—H stretching oscillation of phenols and alcohols [27, 32]. The results confirmed the presence of proteins, polyphenolics, and flavonoids in phytochemical compositions of the DS extract, in particular the presence of Cl^- as a chlorine source for synthesizing Ag/AgCl nanocomposite.

Antibacterial activity of Ag/AgCl nanocomposite

The antibacterial properties of Ag/AgCl nanocomposite were determined by the MIC. It was remarked that the exponential phase of bacteria was delayed in the presence of Ag/AgCl, and this phenomenon was more obvious with an increase of Ag/AgCl concentration (Fig. 6(a)). At the optimal synthesis condition, the Ag/AgCl nanocomposite could delay the exponential phase of MRSA, in which the Ag/AgCl composite could entirely inhibit the growth of MRSA at the MIC of *N*/16 (8.27 mg/L). Furthermore, the antibacterial activity of the Ag/AgCl was defined by the corresponding MBC (Fig. 6(b)), reaching the MBC value of *N*/2 (66.1 mg/L). Besides, the inhibition zone of the Ag/AgCl nanocomposite against MRSA (Fig. 6(c)) revealed the relatively large and uniform inhibition zones at each test (the average inhibition zone diameter of 12.0 mm).

The Ag/AgCl nanocomposite synthesized from DS extract has quite high antibacterial activity against MRSA compared the colloids of AgNPs and graphene oxide-silver nanocomposite as well as the extract of *Quercus infectoria* Olivier nutgalls and leaves, leaves of *Melianthus comosus* Vahl, *Nymphaea lotus* Linn., *Dodonaea angustifolia* (L.f.) Benth (Table 1). Besides that, when the antibacterial zone sizes of the Ag/AgCl nanocomposite and the antibiotics are compared, it is noticeable that the zone size of the nanocomposite sample is approximately equal to that of Erythromycin. Although, the antibacterial zone size of the Ag/AgCl nanocomposite is smaller than that of the antibiotics including Clindamycin, Ciprofloxacin, Gentamicin, and Linezolid as shown in Table 1. But the MIC value of Ag/AgCl nanocomposite green-synthesized using DS extract is much lower than that of all antibiotics. In our study, Ag/AgCl nanocomposite exhibited the

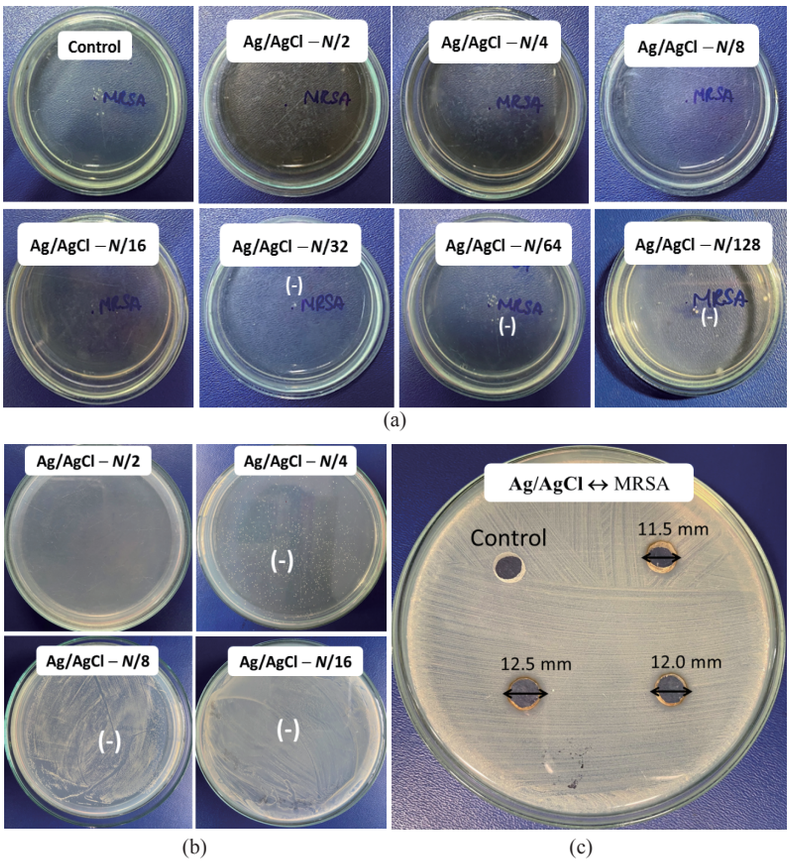

Fig. 6 Images of **(a)** the minimum inhibitory concentration; **(b)** the minimum bactericidal concentration; **(c)** and the inhibition zone of Ag/AgCl nanocomposite (N = 132.2 mg/L) against MRSA

Table 1 Comparison of antibacterial activity of the green-synthesized silver nanoparticles using the DS extract against MRSA with other nanoparticles samples, the plant extracts, and the antibiotics

Sample	IZD (mm)	MIC	MBC	Refs.
Ag/AgCl synthesized by the durian shell extract	12.0	8.27 mg/L	66.1 mg/L	This work
Ag NPs synthesized by *Bacillus subtilis* bacteria	ND	0.23 mg/L	ND	[38]
Ag NPs synthesized with thymol or usnic acid	12.9–13.8	60 μg/L	40–80 mg/L	[39]
Au NPs synthesized from *G. elongata* ethanol extract	16.0	ND	ND	[40]
Ag NPs from Sigma-Aldrich (No. 576832) and Nanoamor No. 0478YD and 0477YD)	ND	0.9–10.8 g/L	2.7–10.8 g/L	[41]
Graphene oxide-silver nanocomposite	ND	31 mg/L	62 mg/L	[42]
Dodonaea angustifolia (L.f.) Benth leaves extract	ND	0.59 g/L	ND	[43]
Melianthus comosus Vahl leaves extract	ND	0.39 g/L	ND	[44]
Nymphaea lotus Linn. leaf extract	8.0–24.0	5.0–10.0 g/L	10–30 g/L	[45]
Quercus infectoria Olivier nutgalls extract	ND	0.4–3.2 g/L	ND	[46]
Clindamycin	15	2 g/L	ND	[47]
Ciprofloxacin	15	5 g/L	ND	[47]
Gentamicin	21	10 g/L	ND	[47]
Erythromycin	12	15 g/L	ND	[47]
Linezolid	21	30 mg/L	ND	[47]

Note: IZD — Inhibition zone diameter; MIC — Minimum inhibitory concentration; MBC — Minimum batericidal concentration; ND- Not done.

higher antibacterial activity, with the addition of AgCl. Besides, the highly uniformed nanoparticles could be also the reason for the outstanding performances. In contrast to commercial antibiotics, nanoparticles may be described by their primary benefits as antibacterial agents since they can operate multiple mechanisms while bacteria cannot gain resistance to these indicated action methods [33]. Furthermore, green-synthesized Ag/AgCl nanocomposite demonstrated minimal or limited cytotoxicity against human dermal fibroblast, easing some of the safety concerns connected with the manufacturing procedure [34]. As a result, Ag/AgCl nanoparticles appear to be trustworthy candidates for safe medicinal uses to prevent MRSA development [35]. The feasibility of utilizing the DS extract for the eco-friendly synthesis of Ag/AgCl nanocomposite highlighted a promising candidate with high antibacterial activity against drug-resistant bacteria.

According to Refs. [36, 37], the use of polymers and nanofibers as a support for silver nanoparticles can help to enhance their antibacterial activity. Therefore, to improve the antibacterial activity of Ag/AgCl nanocomposite as well as overcome the limitation on the silver ion leaching and reduce significantly the cost of the antibacterial products applied on the basis of Ag/AgCl nanocomposite, the in-deep research about the fabrication and the evaluation of the antibacterial activity of Ag/AgCl nanocomposite decorated on polymers and nanofibers also need to be conducted in the next time.

The antibacterial mechanism of Ag/AgCl nanoparticles against MRSA is illustrated in Fig. 7, in which the antibacterial action of Ag/AgCl nanoparticles against MRSA is depicted, such as the direct attachment of Ag/AgCl nanoparticles to the bacterial surface and impacting the membrane's structural integrity [48, 49]. One intriguing mechanism for silver nanoparticle antibacterial action is the production of silver ion (Ag^+), which can denature microbial proteins, interfere with DNA replication, and thus damage bacterial cells [50]. The ROS, which could be produced with a high quantity by Ag/AgCl nanoparticles, is also one of the perpetrators of bacterial growth suppression [51]. The destruction of major cellular components such as protein, DNA, and ribonucleic acid (RNA) caused by oxidative stress results in altered membrane permeability and increased biological component leakage from the cell [52]. The bacteria will suffer permanent oxidative damage and cell death as a result of this [53].

Aside from ROS, reactive nitrogen species (RNS) show promise in destroying harmful bacteria [54]. However, antimicrobial agents based on nanomaterials that can transport and distribute nitric oxide (NO) are extremely scarce and restricted. Aside from ROS and RNS, reactive chlorine species (RCS), which include chlorine gas and chlorine free radicals, play an important role in medical science [55, 56]. The majority of pharmaceuticals on the market are created using chlorine-containing byproducts and contain residual amounts of chlorine [14]. Chlorine is well recognized for its ability to inactivate harmful germs and is commonly employed as a disinfectant in water treatment [14]. Based on the intriguing chlorine chemistry, it is obvious that these highly reactive chlorine free radicals may attack the bacterial cell wall, destroy membrane proteins, impair cellular metabolism, and ultimately cause microbial death

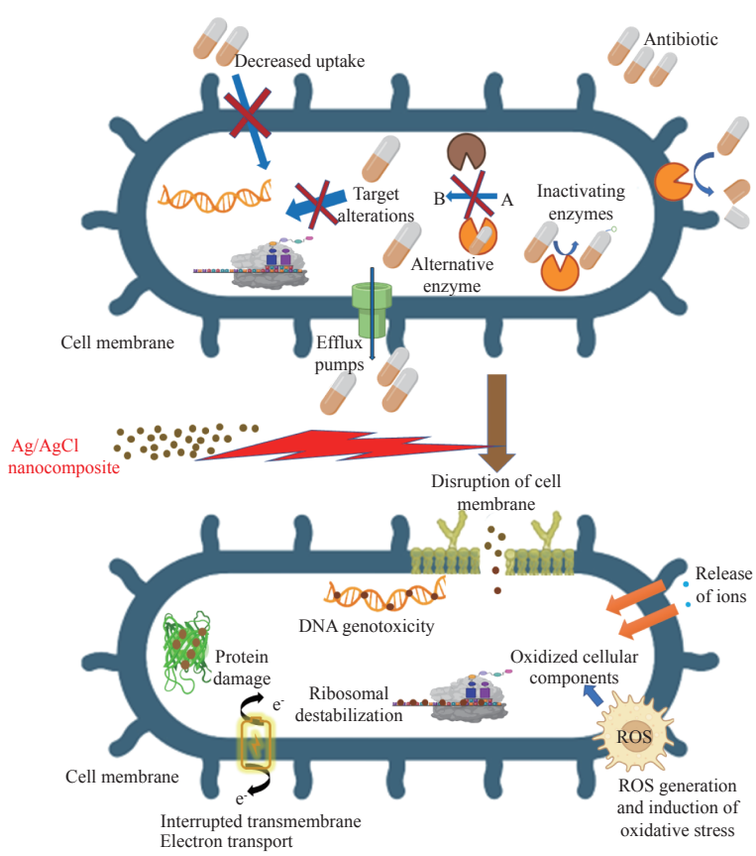

Fig. 7 Illustration of antibacterial mechanism of Ag NPs against methicillin-resistant *Staphylococcus aureus*

[57]. The antibacterial properties of a combination of chlorine (chlorine ligand), silver ions, and tobramycin (chemodrug) were studied in Ref. [58]. The experimental results show that chlorine has a greater bactericidal effect than the other two, i.e., Cl. > Ag^+ > Tobramycin. Furthermore, the combination of Ag^+ ions with Cl. radical can boost the antibacterial actions [59]. While Ag^+ ion has moderate oxidation ability and can attach to the thiol (-SH) groups of several proteins and enzymes, denature and malfunctions of these proteins and enzymes in bacterial cells [60], chlorine free radical is chemically extremely reactive and moderately oxidative, and it can react with several bio-components of bacterial cells [14]. Because they exhibit a variety of ways of action on bacteria, Ag/AgCl nanoparticles are expected to be useful against MRSA.

Conclusion

The extract of durian shell efficiently aided the one-step preparation of Ag/AgCl nanocomposite under light illumination, in compliance with the rules of green synthesis. The phytochemical compositions of the durian shell extract, such as proteins, polyphenolics, and flavonoids, were identified as the main components performing the reduction of silver ions; besides, the presence of chlorine was also beneficial for the formation of AgCl nanoparticles. The crystalline Ag/AgCl nanocomposite with spherical shape and the size range of 15–25 nm was introduced and their high stability in the long-term was attributed to the biomolecules capped on nanoparticles, especially without any additional hazardous agents. The Ag/AgCl nanocomposite demonstrated the great antibacterial potential against methicillin-resistant *Staphylococcus aureus* with the minimum inhibitory concentration of 8.27 mg/L, the minimum bactericidal concentration of 66.1 mg/L and the average inhibition zone diameter of 12.0 mm. To sum up, the present work proposed the facile green synthesis of Ag/AgCl nanoparticles using the extract of durian shell as both reducing and stabilizing agents, against antibiotic-resistant bacteria, typically methicillin-resistant *Staphylococcus aureus*.

Author Contributions

Thi Anh Thu Nguyen: Methodology, Resources, Writing- original draft, Validation, Investigation, Formal analysis. Thi My Thao Nguyen: Methodology, Resources, Validation, Investigation, Formal analysis. Thi Thanh Le Trinh: Methodology, Validation, Investigation, Formal analysis. Van Minh Nguyen: Conceptualization, Methodology, Resources, Writing-original draft, Validation, Investigation, Formal analysis. Nhat Linh Duong: Methodology, Validation, Investigation, Formal analysis. Trung Dang-Bao: Conceptualization, Methodology, Writing - review and editing, Supervision. Tri Nguyen: Conceptualization, Methodology, Writing - review and editing, Supervision.

Conflict of Interests

The authors declare that no competing interest exists.

References

[1] S.H. Podolsky. The evolving response to antibiotic resistance (1945–2018). *Palgrave Commun*, 2018, 4: 124 .https://www.nature.com/articles/s41599-018-0181-x

[2] E. Peterson, P. Kaur. Antibiotic resistance mechanisms in bacteria: Relationships between resistance determinants of antibiotic producers, environmental bacteria, and clinical pathogens. *Frontiers in Microbiology*, 2018, 9: 2928. https://doi.org/10.3389/fmicb.2018.02928

[3] A.S. Lee, H. de Lencastre, J. Garau, et al. Methicillin-resistant *Staphylococcus aureus*. *Nature Reviews Disease Primers*, 2018, 4: 18033. https://doi.org/10.1038/nrdp.2018.33

[4] K.M. Craft, J.M. Nguyen, L.J. Berg, et al. Methicillin-resistant *Staphylococcus aureus* (MRSA): Antibiotic-resistance and the biofilm phenotype. *Med Chem Comm*, 2019, 10: 1231–1241. http://dx.doi.org/10.1039/C9MD00044E

[5] Z.K. Abbas-Al-Khafaji, Q.H. Aubais-aljelehawy. Evaluation of antibiotic resistance and prevalence of multi-antibiotic resistant genes among *Acinetobacter baumannii* strains isolated from patients admitted to al-yarmouk hospital. *Cellular*, *Molecular and Biomedical Reports*, 2021, 1: 60–68. https://doi.org/10.55705/cmbr.2021.142761.1015

[6] N. Asadi, M. Taran, M. Rad, et al. Effects of glucose, metformin, and protein on formation of flower-like nanocomposites of struvite in infected artificial urine medium by methicillin-resistant *Staphylococcus aureus* (MRSA): New report. *Nano Biomedicineand Engineering*, 2019, 11: 91–97. https://doi.org/10.5101/nbe.v11i1.p91-97

[7] M. Alavi, M. Rai. Antisense RNA, the modified CRISPR-Cas9, and metal/metal oxide nanoparticles to inactivate pathogenic bacteria. *Cellular*, *Molecular and Biomedical Reports*, 2021, 1: 52–59. https://doi.org/10.55705/cmbr.2021.142436.1014

[8] M. Rad, M. Taran, M. Alavi. Effect of incubation time, $CuSO_4$ and glucose concentrations on biosynthesis of copper oxide (CuO) nanoparticles with rectangular shape and antibacterial activity: Taguchi method approach. *Nano Biomedicineand Engineering*, 2018, 10: 25–33. https://doi.org/10.5101/nbe.v10i1.p25-33

[9] C.L. Fox Jr, S.M. Modak. Mechanism of silver sulfadiazine action on burn wound infections. *Antimicrob Agents Chemother*, 1974, 5: 582–588. https://doi.org/10.1128/aac.5.6.582

[10] T. Ishida. Antibacterial mechanism of bacteriolyses of

bacterial cell walls by zinc (II) ion induced activations of PGN autolysins, and DNA damages. *Journal of Genes and Proteins*, 2017, 1(1): 1000102.

[11] S.M. Dizaj, F. Lotfipour, M. Barzegar-Jalali, et al. Antimicrobial activity of the metals and metal oxide nanoparticles. *Materials Science and Engineering*: *C*, 2014, 44: 278–284. https://doi.org/10.1016/j.msec.2014.08.031

[12] Chi-Sheng, Chien. Antibacterial activity of silver nanoparticles (AgNP) confined to mesostructured silica against methicillin-resistant *Staphylococcus aureus* (MRSA). *Journal of Alloys and Compounds*, 2018, 747: 1–7. http://dx.doi.org/10.1016/j.jallcom.2018.02.334

[13] S.J. Liao, Y.P. Zhang, X.H. Pan, et al. Antibacterial activity and mechanism of silver nanoparticles against multidrug-resistant *Pseudomonas aeruginosa*. *International Journal of Nanomedicine*, 2019, 14: 1469–1487. https://doi.org/10.2147/ijn.s191340

[14] S. Thangudu, S.S. Kulkarni, R. Vankayala, et al. Photosensitized reactive chlorine species-mediated therapeutic destruction of drug-resistant bacteria using plasmonic core-shell Ag@AgClnanocubes as an external nanomedicine. *Nanoscale*, 2020, 12: 12970–12984. https://doi.org/10.1039/d0nr01300e

[15] A. Hussain, M.F. Alajmi, M.A. Khan, et al. Biosynthesized silver nanoparticle (AgNP) from *Pandanus odorifer* leaf extract exhibits anti-metastasis and anti-biofilm potentials. *Frontiers in Microbiology*, 2019, 10: 8. https://doi.org/10.3389/fmicb.2019.00008

[16] S. Rajput, D. Kumar, V. Agrawal. Green synthesis of silver nanoparticles using Indian *Belladonna* extract and their potential antioxidant, anti-inflammatory, anticancer and larvicidal activities. *Plant Cell Reports*, 2020, 39: 921–939. http://dx.doi.org/10.1007/s00299-020-02539-7

[17] M.P. Patil, J. Palma, N.C. Simeon, et al. *Sasa borealis* leaf extract-mediated green synthesis of silver-silver chloride nanoparticles and their antibacterial and anticancer activities. *New Journal of Chemistry*, 2017, 41: 1363–1371. http://dx.doi.org/10.1039/C6NJ03454C

[18] E.E. Elemike, D.C. Onwudiwe, O.E. Fayemi, et al. Green synthesis and electrochemistry of Ag, Au, and Ag-Au bimetallic nanoparticles using golden rod (*Solidago canadensis*) leaf extract. *Applied Physics A*, 2019, 125: 42. http://dx.doi.org/10.1007/s00339-018-2348-0

[19] N. Kulkarni, U. Muddapur. Biosynthesis of metal nanoparticles: A review. *Journal of Nanotechnology*, 2014, 2014: 510246.https://doi.org/10.1155/2014/510246

[20] N.A. A Aziz, A.M. Mhd Jalil. Bioactive compounds, nutritional value, and potential health benefits of indigenous durian (*Duriozibethinus*Murr.): A review. *Foods*, 2019, 8: 96. https://doi.org/10.3390/foods8030096

[21] A. Manzoor, B. Jan, S. Mehraj, et al. Durian. Antioxidants in fruits: properties and health benefits. Singapore: Springer, 2020: 163–180. https://doi.org/10.1007/978-981-15-7285-2_9

[22] P.A. Nguyen, H.P. Phan, T. Dang-Bao, et al. Sunlight irradiation-assisted green synthesis, characteristics and antibacterial activity of silver nanoparticles using the leaf extract of *Jasminum subtriplinerve Blume*. *Journal of Plant Biochemistry and Biotechnology*, 2022, 31: 202–205. http://dx.doi.org/10.1007/s13562-021-00667-z

[23] D.T. Nguyen, N.L. Duong, V.M. Nguyen, et al. *Chromolaenaodorata* extract as a green agent for the synthesis of Ag@AgCl nanoparticles inactivating bacterial pathogens.*Chemical Papers*, 2020, 74: 1849–1857. http://dx.doi.org/10.1007/s11696-019-01033-z

[24] N.P. Anh, D.N. Linh, N.V. Minh, et al. Positive effects of the ultrasound on biosynthesis, characteristics and antibacterial activity of silver nanoparticles using *Fortunella japonica*. *Materials Transactions*, 2019, 60: 2053–2058. https://doi.org/10.2320/matertrans.m2019065

[25] M. Balouiri, M. Sadiki, S.K. Ibnsouda. Methods for *in vitro* evaluating antimicrobial activity: A review. *Journal of Pharmaceutical Analysis*, 2016, 6: 71–79. https://doi.org/10.1016/j.jpha.2015.11.005

[26] A. Moosa, A.M. Ridha, M. Al-Kaser. Process parameters for green synthesis of silver nanoparticles using leaves extract of *Aloe*vera plant. *International Journal of Multidisciplinary and Current Research*, 2015, 3: 966–975.

[27] Y. Gopalakrishnan, A. Al-Gheethi, M. Abdul Malek, et al. Removal of basic brown 16 from aqueous solution using durian shell adsorbent, optimisation and techno-economic analysis. *Sustainability*, 2020, 12: 8928. https://doi.org/10.3390/su12218928

[28] U. Holzwarth, N. Gibson. The Scherrer equation versus the 'Debye-Scherrer equation'. *Nature Nanotechnology*, 2011, 6: 534.https://doi.org/10.1038/nnano.2011.145

[29] R. Sattari, G.R.Khayati, R. Hoshyar. Biosynthesis and characterization of silver nanoparticles capped by biomolecules by *Fumaria parviflora* extract as green approach and evaluation of their cytotoxicity against human breast cancer MDA-MB-468 cell lines. *Materials Chemistry and Physics*, 2020, 241: 122438. http://dx.doi.org/10.1016/j.matchemphys.2019.122438

[30] V. Ahluwalia, S. Elumalai, V. Kumar, et al. Nano silver particle synthesis using *Swertiapaniculata* herbal extract and its antimicrobial activity. *Microbial Pathogenesis*, 2018, 114: 402–408. https://doi.org/10.1016/j.micpath.2017.11.052

[31] V. Ahluwalia, J. Kumar, R. Sisodia, et al. Green synthesis of silver nanoparticles by *Trichoderma harzianum* and their bio-efficacy evaluation against *Staphylococcus aureus* and *Klebsiella pneumonia*. *Industrial Crops and Products*, 2014, 55: 202–206. http://dx.doi.org/10.1016/j.indcrop.2014.01.026

[32] R. Sattari, G.R. Khayati, R. Hoshyar. Biosynthesis of silver-silver chloride nanoparticles using fruit extract of *Levisticumofficinale*: Characterization and anticancer activity against MDA-MB-468 cell lines. *Journal of Cluster Science*, 2021, 32: 593–599. http://dx.doi.org/10.1007/s10876-020-01818-3

[33] N. Filipović, D. Ušjak, M.T. Milenković, et al. Comparative study of the antimicrobial activity of selenium nanoparticles with different surface chemistry and structure. *Frontiers in Bioengineering and Biotechnology*, 2021, 8: 624621. https://doi.org/10.3389/fbioe.2020.624621

[34] D. Medina Cruz, G. Mi, T.J. Webster. Synthesis and characterization of biogenic selenium nanoparticles with antimicrobial properties made by *Staphylococcus aureus*, methicillin-resistant *Staphylococcus aureus* (MRSA), *Escherichia coli*, and *Pseudomonas aeruginosa*. *Journal of Biomedical Materials Research Part A*, 2018, 106: 1400–1412. https://doi.org/10.1002/jbm.a.36347

[35] Mahendra, Rai. Broadening the spectrum of small-molecule antibacterials by metallic nanoparticles to overcome microbial resistance. *International Journal of Pharmaceutics*, 2017, 532: 139–148. http://dx.doi.org/10.1016/j.ijpharm.2017.08.127

[36] M.I. Shekh, D.M. Patel, K.P. Patel, et al. Electrospun nanofibers of poly(NPEMA-co.-CMPMA): Used as heavy metal ion remover and water sanitizer. *Fibers and Polymers*, 2016, 17: 358–370. http://dx.doi.org/10.1007/s12221-016-5861-9

[37] M.I. Shekh, N.N. Patel, K.P. Patel, et al. Nano silver-embedded electrospun nanofiber of poly(4-chloro-3-methylphenyl methacrylate): use as water sanitizer. *Environmental Science and Pollution Research*, 2017, 24: 5701–5716. https://doi.org/10.1007/s11356-016-8254-0

[38] K.I. Alsamhary. Eco-friendly synthesis of silver nanoparticles by *Bacillus subtilis* and their antibacterial activity. *Saudi Journal of Biological Sciences*, 2020, 27:

2185–2191. https://doi.org/10.1016/j.sjbs.2020.04.026

[39] M. Alavi, N. Karimi. Biosynthesis of Ag and Cu NPs by secondary metabolites of usnic acid and thymol with biological macromolecules aggregation and antibacterial activities against multi drug resistant (MDR) bacteria. *International Journal of Biological Macromolecules*, 2019, 128: 893–901. https://doi.org/10.1016/j.ijbiomac.2019.01.177

[40] N. Abdel-Raouf, N.M. Al-Enazi, I.B.M. Ibraheem. Green biosynthesis of gold nanoparticles using *Galaxauraelongata* and characterization of their antibacterial activity. *Arabian Journal of Chemistry*, 2017, 10: S3029–S3039. http://dx.doi.org/10.1016/j.arabjc.2013.11.044

[41] N.V. Ayala-Núñez, H.H. Lara Villegas, L. del Carmen IxtepanTurrent, et al. Silver nanoparticles toxicity and bactericidal effect against methicillin-resistant *Staphylococcus aureus*: Nanoscale does matter. *Nanobiotechnology*, 2009, 5: 2–9. http://dx.doi.org/10.1007/s12030-009-9029-1

[42] A.C. de Moraes, B.A. Lima, A.F. de Faria, et al. Graphene oxide-silver nanocomposite as a promising biocidal agent against methicillin-resistant *Staphylococcus aureus*. *International Journal of Nanomedicine*, 2015, 10: 6847–6861. https://doi.org/10.2147/ijn.s90660

[43] H.M. Heyman, A.A. Hussein, J.J.M. Meyer, et al. Antibacterial activity of South African medicinal plants against methicillin resistant *Staphylococcus aureus*. *Pharmaceutical Biology*, 2009, 47: 67–71. http://dx.doi.org/10.1080/13880200802434096

[44] S.P.N. Mativandlela, J.J.M. Meyer, A.A. Hussein, et al. Antitubercular activity of compounds isolated from *Pelargonium sidoides*. *Pharmaceutical Biology*, 2007, 45: 645–650. https://doi.org/10.1080/13880200701538716

[45] O.J. Akinjogunla, C. Yah, N. Eghafona, et al. Antibacterial activity of leave extracts of *Nymphaea* lotus (Nymphaeaceae) on methicillin resistant *Staphylococcus aureus* (MRSA) and vancomycin resistant *Staphylococcus aureus* (VRSA) isolated from clinical samples. *Annals of Biological Research*, 2010, 1: 174–184.

[46] G. Sucilathangam, S. Gomatheswari, G. Velvizhi et al. Detection of anti-bacterial activity of medicinal plant Quercus infectoria against MRSA isolates in clinical samples. *Journal of Pharmaceutical and Biomedical Sciences*, 2012, 14(8): 1–4.

[47] B. Manipriya, T. Banu, P. Kumar L, et al. Evaluation of antibacterial activity of silver nanoparticles against methicillin-resistant *Staphylococcus aureus* and detection of virulence factors - nuclease, phosphatase, and bio film production. *Asian Journalof Pharmaceutical and Clinical Research*, 2018, 11: 224. https://doi.org/10.22159/ajpcr.2018.v11i5.24097

[48] A. Ronen, W.Y. Duan, I. Wheeldon, et al. Microbial attachment inhibition through low-voltage electrochemical reactions on electrically conducting membranes. *Environmental Science&Technology*, 2015, 49: 12741–12750. https://doi.org/10.1021/acs.est.5b01281

[49] K. Okaiyeto, M.O. Ojemaye, H. Hoppe, et al. Phytofabrication of silver/silver chloride nanoparticles using aqueous leaf extract of *Oederagenistifolia*: Characterization and antibacterial potential. *Molecules*, 2019, 24: 4382. https://doi.org/10.3390/molecules24234382

[50] Y.H. Hsueh, K.S. Lin, W.J. Ke, et al. The antimicrobial properties of silver nanoparticles in *Bacillus subtilis* are mediated by released Ag^+ ions. *PLoSONE*, 2015, 10: e0144306. https://doi.org/10.1371/journal.pone.0144306

[51] F.N. Spagnoletti, C. Spedalieri, F. Kronberg, et al. Extracellular biosynthesis of bactericidal Ag/AgCl nanoparticles for crop protection using the fungus *Macrophominaphaseolina*. *Journal of Environmental Management*, 2019, 231: 457–466. https://doi.org/10.1016/j.jenvman.2018.10.081

[52] C.H.N. Barros, S. Fulaz, D. Stanisic, et al. Biogenic nanosilver against multidrug-resistant bacteria (MDRB). *Antibiotics*, 2018, 7: 69. https://doi.org/10.3390/antibiotics7030069

[53] Y.S. Raval, A. Mohamed, H.M. Zmuda, et al. Hydrogen-peroxide-generating electrochemical scaffold eradicates methicillin-resistant *Staphylococcus aureus* biofilms. *Global Challenges*, 2019, 3: 1800101. https://doi.org/10.1002/gch2.201800101

[54] F.C. Fang. Antimicrobial reactive oxygen and nitrogen species: Concepts and controversies. *Nature Reviews Microbiology*, 2004, 2: 820–832. https://doi.org/10.1038/nrmicro1004

[55] P.P. Li, H.X. Wu, A. Dong. Ag/AgX nanostructures serving as antibacterial agents: Achievements and challenges. *Rare Metals*, 2022, 41: 519–539. http://dx.doi.org/10.1007/s12598-021-01822-0

[56] A. Valavanidis, T. Vlachogianni, K. Fiotakis, et al. Pulmonary oxidative stress, inflammation and cancer: Respirable particulate matter, fibrous dusts and ozone as major causes of lung carcinogenesis through reactive oxygen species mechanisms. *International Journal of Environmental Research and Public Health*, 2013, 10: 3886–3907. https://doi.org/10.3390/ijerph10093886

[57] M. Saran, I. Beck-Speier, B. Fellerhoff, et al. Phagocytic killing of microorganisms by radical processes: Consequences of the reaction of hydroxyl radicals with chloride yielding chlorine atoms. *Free Radical Biology and Medicine*, 1999, 26: 482–490. https://doi.org/10.1016/s0891-5849(98)00187-7

[58] J. Kim, B. Pitts, P.S. Stewart, et al. Comparison of the antimicrobial effects of chlorine, silver ion, and tobramycin on biofilm. *Antimicrobial Agents and Chemotherapy*, 2008, 52: 1446–1453. https://doi.org/10.1128/aac.00054-07

[59] C.Y. Mao, Y.M. Xiang, X.M. Liu, et al. Photo-inspired antibacterial activity and wound healing acceleration by hydrogel embedded with Ag/Ag@AgCl/ZnO nanostructures. *ACS Nano*, 2017, 11: 9010–9021. https://doi.org/10.1021/acsnano.7b03513

[60] Z. Qin, Y. Zheng, Y. Wang, et al. Versatile roles of silver in Ag-based nanoalloys for antibacterial applications. *Coordination Chemistry Reviews*, 2021, 449: 214218. http://dx.doi.org/10.1016/j.ccr.2021.214218